JOURNAL OF CATALYSIS 112, 478–488 (1988)

Ethane Hydrogenolysis and Hydrogen Chemisorption over Niobia-Promoted Rhodium Catalysts: A New Phase by a Strong Rhodium–Niobia Interaction

Z. HU, H. NAKAMURA, K. KUNIMORI,[1] H. ASANO, AND T. UCHIJIMA[1]

Institute of Materials Science, University of Tsukuba, Tsukuba, Ibaraki 305, Japan

Received January 4, 1988; revised March 14, 1988

Niobia-promoted Rh/SiO_2 catalysts, containing niobia (Nb_2O_5) deposited onto Rh/SiO_2 catalysts, exhibited chemical behavior characteristic of strong metal–support interaction, the $Rh–Nb_2O_5$ interaction being as strong as that in the Rh/Nb_2O_5 system. In a typical case, after the high-temperature reduction at 773 K, the H_2 chemisorption ability diminished almost to zero and the catalytic activity for ethane hydrogenolysis decreased by about seven orders of magnitude, compared with the low-temperature reduction (LTR) at 373 K. The phenomenon is reversed after the oxidation in O_2 at 673 K followed by LTR. The extent of $Rh–Nb_2O_5$ interaction was sensitive to preparation variables such as the amount of Nb_2O_5 deposited and preparation method. In particular, the extent of interaction was increased significantly by calcining Nb_2O_5-promoted Rh catalysts in air at high temperatures (973 K). An X-ray diffraction study suggested formation of a new phase ($RbNbO_4$) by the calcination treatment at 973 K. Temperature-programmed reduction results showed that the reduction peaks shifted to the higher temperature side as the degree of the $Rh–Nb_2O_5$ interaction increased. A model for the metal–oxide interaction in the present catalyst system is discussed in terms of the formation of a surface $RhNbO_4$ compound and the decoration of the Rh surface with a niobia species (NbO_x).

INTRODUCTION

The work of Tauster and co-workers (*1, 2*) has stimulated numerous studies of strong metal–support interaction (SMSI) effects on the chemisorption and catalytic properties of metal catalysts supported on TiO_2 and reducible oxides. Recently, a model involving migration of reduced species of the support onto metal particles which results in a geometric effect (*3, 4*) has been proposed to interpret the SMSI phenomena, and several studies of model catalysts have provided direct physical evidences for the covering of the metal surface with an oxide species (e.g., TiO_x) in various catalysts ("decoration model") (*5–9*).

SMSI oxides (TiO_2, MnO, V_2O_3, Nb_2O_5, etc.) have also been used as a promoter in metal catalysts supported on non-SMSI oxides (e.g., SiO_2). The promotion effects of TiO_2, MnO, Nb_2O_5, etc., have been reported in CO hydrogenation, etc., on Rh/SiO_2 (*10–13*) and Pd/SiO_2 (*14, 15*) catalysts. Since the catalytic properties of the catalysts are modified drastically by the oxide promoter, the interaction between metal and SMSI oxide is of considerable interest. Motivated by the similarity between SMSI (the decoration model) and the metal–oxide additive effects, some attempts have been made to study SMSI behavior using a SMSI oxide deposited onto a non-SMSI oxide (SiO_2 or Al_2O_3) as catalyst support (*16–19*). However, the interaction was not as strong as that exerted by the bulk SMSI oxides.

We have recently shown that a niobia-promoted Rh catalyst, containing niobia (Nb_2O_5) deposited onto a Rh/SiO_2 catalyst, exhibited SMSI behavior in ethane hydrogenolysis studies. The $Rh–Nb_2O_5$ interaction was as strong as that in the Rh/Nb_2O_5 system (*20, 21*); i.e., the catalytic activity decreased drastically with increasing cata-

[1] To whom correspondence should be addressed.

0021-9517/88 $3.00

lyst reduction temperature (e.g., depression of about seven orders of magnitude after high-temperature reduction (HTR) at 773 K compared with low-temperature reduction (LTR) at 373 K). The acronym "SMSI behavior" is used here for the cases which meet the definition in the original observations (*1, 2*); i.e., a drastic suppression of chemisorption ability and/or catalytic activity after high-temperature reduction and its recovery after high-temperature O_2 treatment followed by low-temperature reduction (*16–18*). Although the SMSI behavior has been amply confirmed in their original catalyst system (metal/TiO_2, metal/Nb_2O_5, etc.), new catalyst systems including Nb_2O_5-promoted Rh catalysts have been observed to exhibit equivalent behavior (*16–20*).

In this paper, the results of our recent work with the Nb_2O_5-promoted Rh/SiO_2 catalysts will be presented. Hydrogen chemisorption and ethane hydrogenolysis reaction were used as chemical probes for the degree of the Rh–Nb_2O_5 interaction, and the catalysts were characterized by temperature-programmed reduction (TPR) and X-ray diffraction (XRD) measurements. During the course of the study, we have found that the extent of the metal–oxide interaction was increased by the calcination of the Nb_2O_5-promoted Rh catalysts in air at a high temperature (*22*). Therefore, in the present paper we focus our attention on the effect of the calcination treatment. The results of H_2 chemisorption and ethane hydrogenolysis reaction will first be described, followed by the characterization with TPR and XRD and a discussion about a possible model of metal–oxide interaction in the Nb_2O_5-promoted Rh/SiO_2 catalysts.

EXPERIMENTAL

Preparation of Catalysts

A 0.5 wt% Rh/SiO_2 catalyst (JRC-SIO-3-0.5Rh) was provided as Japan Reference Catalyst (JRC) (*23*). A 5.0 wt% Rh/SiO_2 catalyst was prepared by impregnating the SiO_2 support (JRC-SIO-3, BET surface area of 186 m^2/g) with an aqueous solution of $RhCl_3$ to incipient wetness. The impregnated sample was dried at 393 K overnight and reduced in H_2 flow at 773 K for 1 h.

The Nb_2O_5-promoted 0.5 wt% Rh/SiO_2 catalysts were prepared by the incipient wetness impregnation of 0.5 wt% Rh/SiO_2 catalyst, which had been calcined in air at 773 K, with an aqueous solution of $(NH_4)_3(NbO(C_2O_4)_3)$, and then the catalyst was dried at 393 K overnight and calcined at 773 K for 1 h to decompose the niobia precursor. The Nb_2O_5 loading was about 0.57, 5.7, and 6.8 wt%, corresponding to Nb/Rh atomic ratios of 0.88, 9.3, and 11.4, respectively. This series of catalysts is designated catalyst A. The Nb_2O_5-promoted 5.0 wt% Rh/SiO_2 (Nb/Rh = 3.1) was obtained by impregnation of 5.0 wt% Rh/SiO_2 catalyst with a solution of $NbCl_5$ dissolved in ethanol, followed by degassing *in vacuo* for 6 h to remove the ethanol solvent and calcining in air at 773 K for 1 h to decompose the niobia precursor. This catalyst was designated catalyst B.

In another preparation method, the SiO_2 support (JRC-SIO-3) was impregnated with a solution of $(NH_4)_3(NbO(C_2O_4)_3)$ and dried at 393 K overnight. The resulting support (5.7 wt% Nb_2O_5/SiO_2) was calcined at 973 K for 3 h to sinter the niobia to a larger crystalline. The 0.5 wt% Rh/Nb_2O_5/SiO_2 catalyst (designated catalyst C) was obtained from this support by its impregnation with an aqueous $RhCl_3$ solution and dried at 393 K overnight followed by reduction in H_2 flow at 773 K for 1 h.

Hydrogen Chemisorption

The volumetric adsorption of H_2 was studied by a conventional glass vacuum system (*24*), base pressure of 10^{-5} to 10^{-6} Torr (1 Torr = 133.3 N m^{-2}) being attained by an oil diffusion pump with a liquid nitrogen trap. Reduced catalyst samples of 0.2 to 0.3 g were placed in a Pyrex tube. The amounts of gas adsorbed on the catalysts were determined from pressure mea-

surements with an MKS Baratron pressure gauge. Dead volumes were calibrated using helium gas. The isotherms were not studied in detail, but the adsorption measurements were performed at room temperature and the lower equilibrium pressures (about 8 Torr). The adsorption of H_2 at room temperature was instantaneous. However, it was followed by a slow gas uptake, the rate of which became negligible after 1 h. Therefore, typically, the amount of the uptake was measured at 1 h after the admission of H_2 gas. The catalyst was pretreated for 1 h in O_2 flow at 673 K, followed by reduction at the desired temperature in H_2 flow purified through a zeolite bed at liquid nitrogen temperature, and then evacuated *in vacuo* at the catalyst reduction temperature before the measurement of H_2 adsorption. The amount of H_2 chemisorption was expressed in terms of H/Rh (the number of chemisorbed H atoms/the total number of Rh atoms in the catalyst).

Ethane Hydrogenolysis

The catalytic activity measurements for the ethane hydrogenolysis reaction were performed in a microcatalytic pulse reactor (*21*). The catalyst (1.0 g) was placed in a Pyrex tube connected to stainless-steel piping by swagelok fittings. Purified He gas was used as the carrier gas (flow rate, 70 cm^3/min) and a pulse (1 cm^3) of a mixture gas (C_2H_6, 2.7%; H_2, 31.8%; He balance) was injected by a jacketed switching valve purged with He. The impurity level of the carrier gas was less than 0.05 ppm in O_2. Analysis was performed by an on-line gas chromatograph. The reaction rate was calculated from the conversion and a residence time (assumed to be the catalyst bed volume in a ratio to the carrier flow rate) (*25*) and expressed in molecules converted per total Rh atoms per second.

Temperature-Programmed Reduction

The TPR measurements were performed in a flow system with the catalyst (0.25 g) placed in a microreactor connected to a quadrupole mass spectrometer (QMS, ANELVA TE-150). After the catalyst was calcined in O_2 flow (30 cm^3/min) at 673 K for 1 h, it was purged with He gas up to 773 K to remove any possible oxygen adsorbate over the support. The sample was subsequently cooled in He to room temperature, then a mixture of 1120 ppm H_2 in He was passed through the catalyst bed at 30 cm^3/min, and the H_2 consumption was monitored as the catalyst temperature was raised at 5 or 20 K/min up to 773 K.

TABLE 1

The Results of H_2 Adsorption, XRD, and TEM for the Nb_2O_5-Promoted and Unpromoted Rh/SiO_2 Catalysts

Catalyst	Nb/Rh[a]	H_2 adsorption[b] (H/Rh)	Rh particle size (nm)	
			From XRD	From TEM
0.5% Rh/SiO_2	0.0	0.35	—	3.2
Catalyst A	9.3	0.25	—	—
5.0% Rh/SiO_2	0.0	0.20	5.5	4.5
Catalyst B	3.1	0.11	5.2	—

[a] The atomic ratio of Nb to Rh.

[b] The total H_2 uptake after the H_2 reduction at 373 K. For details, see Figs. 1 and 2.

TEM and XRD

The transmission electron microscopy (TEM) measurements were performed with a JEOL JEM 120CX instrument. TEM samples were prepared by placing a drop of a suspension of finely meshed particles in toluene on a copper grid (*26*). An X-ray diffractometer (Rigaku Co., Ltd.) equipped with a graphite monochromator for Cu$K\alpha$ radiation (40 kV, 30 mA) was used for the X-ray diffraction studies. The mean Rh particle size was calculated from the line-broadening measurement, as described elsewhere (*26*).

RESULTS

Rh Dispersion

The Rh particle sizes of the catalysts based on TEM and XRD studies are given in Table 1. For the unpromoted Rh/SiO_2 catalysts, the Rh dispersions (the H/Rh

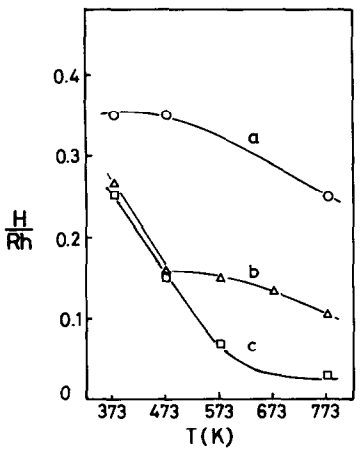

FIG. 1. Effect of catalyst reduction temperature on the capacities of H_2 adsorption for the Nb_2O_5-promoted 0.5% Rh/SiO_2 catalysts. (a) Rh/SiO_2, 0.5%; (b) catalyst A (Nb/Rh = 0.9); (c) the catalyst A (Nb/Rh = 9.3).

values) from H_2 adsorption measurements are in reasonable agreement with those determined by TEM and XRD. As indicated by the XRD results in Table 1, no change in the mean Rh particle size was observed between the unpromoted 5.0 wt% Rh/SiO_2 and the Nb_2O_5-promoted Rh/SiO_2 (catalyst B). However, the H/Rh values of the Nb_2O_5-promoted Rh/SiO_2 catalysts (A and B) were significantly less than those of the corresponding unpromoted Rh/SiO_2 catalysts, respectively. This result suggests that the Rh surface in the promoted catalysts was partially covered with the Nb_2O_5 promoter even after the low-temperature reduction at 373 K.

H_2 Chemisorption

Figure 1 shows the variation in the H_2 uptake for the unpromoted and Nb_2O_5-promoted 0.5% Rh/SiO_2 catalysts as a function of catalyst reduction temperature. For the 0.5% Rh/SiO_2 catalyst, a small decrease in the H/Rh value was observed after the high-temperature reduction at 773 K, but the capacity of H_2 adsorption was suppressed much more significantly for the Nb_2O_5-promoted Rh/SiO_2 (catalyst A). The effect was more drastic for the catalyst A with an Nb/Rh value of 9.3 than that with a value of 0.9. In the former case, the H/Rh value diminished to almost zero after high-temperature reduction at 773 K. The H_2 adsorption data for the unpromoted 5.0 wt% Rh/SiO_2 and the Nb_2O_5-promoted 5.0% Rh/SiO_2 (catalyst B) are given in Fig. 2. For the 5.0% Rh/SiO_2 catalyst, the H/Rh value was independent of catalyst reduction temperature. In catalyst B, however, substantial suppression of H_2 adsorption ability was observed with increasing catalyst reduction temperature. The H/Rh value diminished almost to zero even after reduction at 573 K.

The H_2 adsorption ability for catalyst C, which was prepared from the 5.7 wt% Nb_2O_5/SiO_2 calcined at 973 K, is shown in Fig. 3 as a function of catalyst reduction temperature. When catalyst C was reduced at temperatures lower than 573 K, the H/Rh value decreased with increasing catalyst reduction temperature, but no further decrease in the H/Rh value was shown at the higher temperatures up to 773 K. The effect of the calcination treatment at high temperatures (973 K) is also shown in Fig. 3. After catalyst C was calcined in air at 973

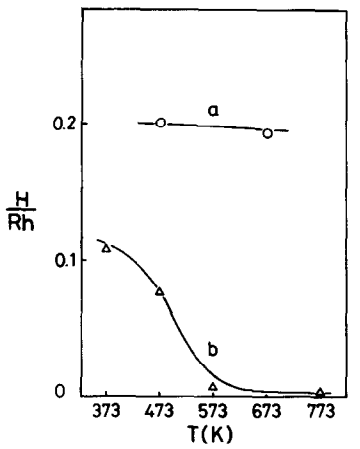

FIG. 2. Effect of catalyst reduction temperature on the capacities of H_2 adsorption for the Nb_2O_5-promoted 5.0% Rh/SiO_2 catalysts. (a) Rh/SiO_2, 5.0%; (b) catalyst B.

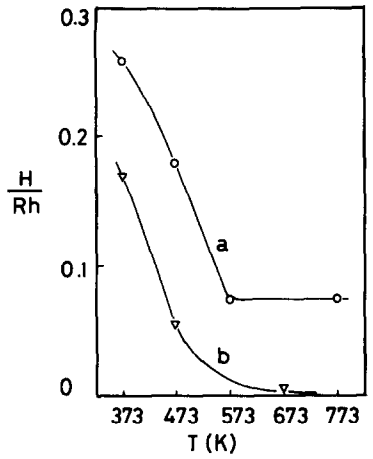

FIG. 3. Effect of catalyst reduction temperature on the capacity of H_2 adsorption for catalyst C. (a) Catalyst C calcined at 773 K; (b) catalyst C calcined at 973 K.

K, more severe suppression in the uptake of H_2 was observed with increasing catalyst reduction temperature. The H/Rh value diminished to zero after reduction at 673 K.

Ethane Hydrogenolysis

Figure 4 shows the Arrhenius plots of ethane hydrogenolysis activity for catalyst A (Nb/Rh = 11.4). The catalytic activity decreased drastically; i.e., the reaction temperature to gain observable conversion range (3 to 10%) increased with increasing catalyst reduction temperature. For example, to get the rate of 0.01 molecule/(total Rh atom sec), the reaction temperature was 446 K for the catalyst reduced at 473 K (curve a), while the reaction temperature of 763 K was needed after the catalyst was reduced at 773 K (curve b). It should be noted that the phenomenon was reversible; i.e., the catalytic activity was restored, if the catalyst was treated in O_2 at 673 K followed by the low-temperature reduction (see curve c in Fig. 4). Similar reversible phenomena were also observed in the ethane hydrogenolysis studies on catalysts B and C. The activation energy appeared to be almost constant (35 kcal/mol) among the data at different catalyst reduction temperatures.

Figure 5 shows the catalytic activity for ethane hydrogenolysis as a function of catalyst reduction temperature. The activities were calculated for 435 K from Arrhenius plots simply to allow a ready comparison among different reduction temperatures. For catalyst A (Nb/Rh = 9.3, 11.4), the catalytic activity decreased by about seven orders of magnitude after high-temperature reduction at 773 K, relative to the low-temperature reduction at 373 K. The suppres-

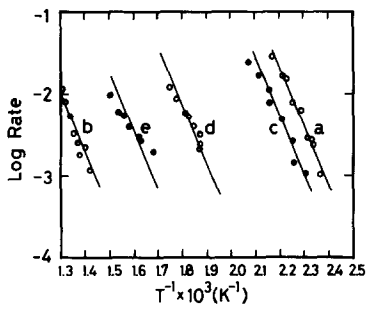

FIG. 4. Comparison of the ethane hydrogenolysis activities for catalyst A (Nb/Rh = 11.4) reduced at different temperatures. Reduction at (a) 473 K, (b) 773 K, (c) 473 K, (d) 573 K, and (e) 673 K. Before each reduction treatment, the catalyst was pretreated in O_2 at 673 K.

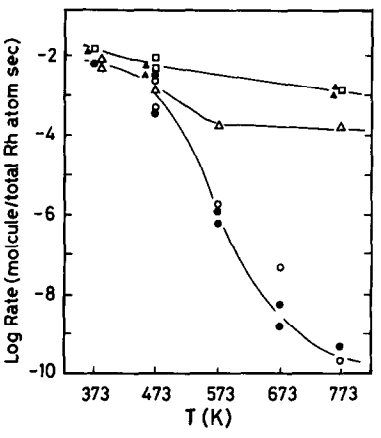

FIG. 5. Effect of catalyst reduction temperature on the catalytic activity for ethane hydrogenolysis. (□) Rh/SiO_2, 0.5%; (▲) physical mixing of 0.5% Rh/SiO_2 with Nb_2O_5 oxide; (△) catalyst A (Nb/Rh = 0.9); (●) catalyst A (Nb/Rh = 9.3); (○) catalyst A (Nb/Rh = 11.4).

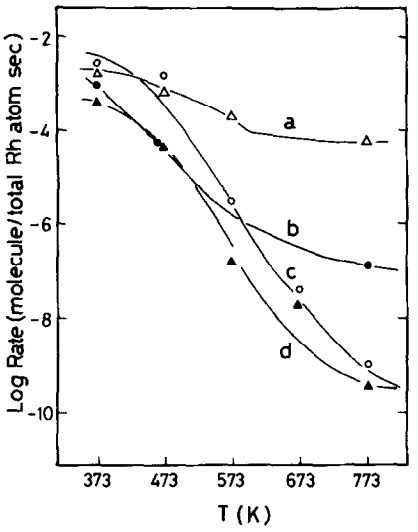

FIG. 6. Effect of calcination at high temperatures on the catalytic activities for ethane hydrogenolysis on the Nb_2O_5-promoted Rh/SiO_2 catalysts. (a) Catalyst C calcined at 773 K; (b) catalyst B calcined at 773 K; (c) catalyst B calcined at 973 K; (d) catalyst C calcined at 973 K.

sion extent is comparable to that in the 0.5% Rh/Nb_2O_5 catalyst (*21*). For the catalyst A with the lower loading of Nb_2O_5 (Nb/Rh = 0.9), the effect of catalyst reduction temperature on the catalytic activity was less pronounced. The observed decrease in the activity of the Nb_2O_5-promoted catalysts is due to the Nb_2O_5 promoter, because no drastic change of the catalytic activity was observed in the unpromoted 0.5 wt% Rh/SiO_2 catalyst. As also shown in Fig. 5, its physical mixing with the Nb_2O_5 oxide was insufficient to cause the SMSI behavior.

Figure 6 shows the catalytic activity for ethane hydrogenolysis over catalysts B and C as a function of catalyst reduction temperature. For catalyst C, the catalytic activity after HTR was suppressed only by 1.5 orders of magnitude compared with that after LTR at 373 K. The effect of the calcination treatment at the high temperature was observed on the catalytic behavior. The calcination of catalyst C in air at 973 K caused the drastic decrease in the catalytic activity with increasing catalyst reduction temperature (depression of the activity of about 6 orders of magnitude after HTR relative to LTR at 373 K). For catalyst B, the catalytic activity decreased by about 4 orders of magnitude after HTR at 773 K relative to LTR at 373 K. The effect of the calcination was also observed in catalyst B (see Fig. 6). After catalyst B was calcined in air at 973 K, more significant suppression was observed; i.e., the catalytic activity decreased by ca. 7 orders of magnitude after HTR at 773 K.

Temperature-Programmed Reduction

TPR experiments were performed to characterize the reducibility of the unpromoted and Nb_2O_5-promoted Rh/SiO_2 catalysts. As shown in Fig. 7, the TPR spectrum of the 0.5% Rh/SiO_2 catalyst consists of a sharp peak centered at 350 K with a small tail up to 423 K. For the Nb_2O_5-promoted Rh catalysts, however, the H_2 consumption was observed in a wide range of temperature up to 773 K during the TPR. The TPR spectrum of catalyst A with the Nb/Rh value of 0.9 is much more complex than that of the 0.5 wt% Rh/SiO_2 catalyst. The spectrum contains reduction peaks at

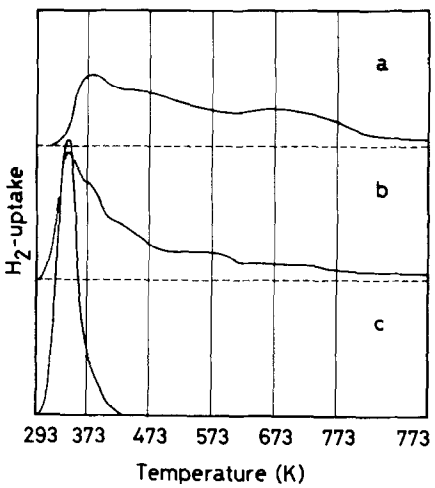

FIG. 7. TPR spectra of the Nb_2O_5-promoted 0.5% Rh/SiO_2 catalysts. (a) Catalyst A (Nb/Rh = 9.3); (b) catalyst A (Nb/Rh = 0.9); (c) 0.5% Rh/SiO_2 catalyst. Catalyst temperature was ramped at 5 K/min.

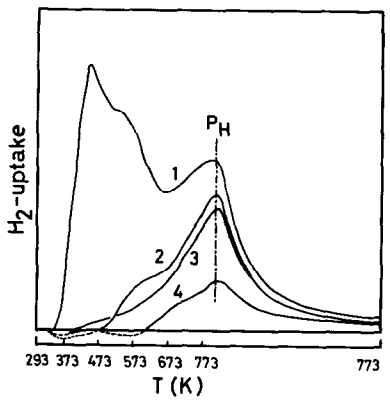

FIG. 8. TPR spectra of catalyst A (Nb/Rh = 9.3) after different pretreatments. (1) Calcined in O_2 at 673 K, then flushed in He up to 773 K; (2) after (1), the catalyst was reduced in H_2 at 373 K; (3) after (1), the catalyst was reduced at 373 K, then flushed in He up to 773 K; (4) after (1), the catalyst was reduced at 473 K. Catalyst temperature was ramped at 20 K/min.

the higher-temperature side, but the peak centered at 350 K is still the main one. In the catalyst A with the Nb/Rh value of 9.3, all of the reduction peaks have shifted to the higher-temperature side in comparison with those in the 0.5% Rh/SiO_2 catalyst. It is noted that no H_2 consumption was observed up to 773 K during the TPR of the 5.7 wt% Nb_2O_5/SiO_2 support.

To characterize the interaction between Rh and Nb_2O_5 in more detail, the TPR spectra of catalyst A (Nb/Rh = 9.3) after various pretreatments were studied as shown in Fig. 8 (20 K/min). The TPR spectrum of the catalyst treated in O_2 at 673 K (TPR 1) may be divided roughly into two parts: the H_2 consumptions at the lower- and higher-temperature sides. For the catalyst reduced in H_2 at 373 K, only the peak of P_H (the reduction peak at the higher-temperature side) was observed (see TPR 2) and no significant effect of the He treatment at 773 K was observed (TPR 3). After the H_2 reduction at 473 K, the peak of P_H was still observed during the TPR measurement (see TPR 4), although the amount of the H_2 consumption decreased substantially. These results suggest that the peak at the lower-temperature side is due to the reduction of Rh oxide, and the peak at the higher-temperature side (P_H) corresponds to a strongly interacting part between Rh and Nb_2O_5.

Figures 9 and 10 show the effect of the calcination treatment at high temperatures on TPR spectra. The TPR spectra of catalyst B (Fig. 9) showed that the reduction peaks shifted to higher temperatures by increasing the catalyst calcination temperature (from 773 to 973 and 1173 K). As shown in Fig. 10a, the TPR spectrum of catalyst C after the O_2 treatment at 673 K exhibits a broad peak at ca. 400 K with a tail extending to the higher temperature. After catalyst C was calcined in air at 973 K, the contribution of the reduction peaks at the higher temperatures increased remarkably, as shown in Fig. 10b. Following the measurement (b), the TPR spectrum was measured after the O_2 treatment at 673 K, as given in Fig. 10c. The TPR spectrum (c) still exhibits the reduction peaks at the higher temperatures, although the peak at around 730 K diminished substantially. The comparison of spectrum (c) with (a) in Fig. 10 revealed that a more strongly interacting

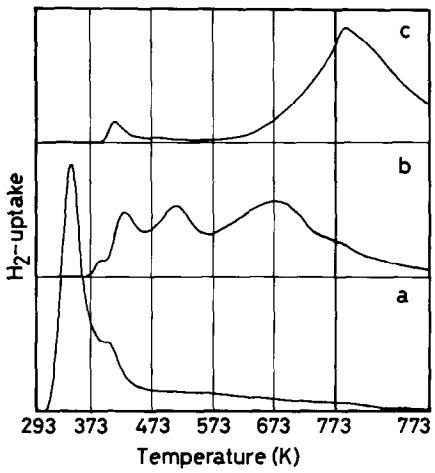

FIG. 9. Effect of calcination temperature on the TPR spectra of the catalyst B. (a) Calcined in O_2 at 773 K; (b) calcined in air at 973 K; (c) calcined in air at 1173 K. Catalyst temperature was ramped at 5 K/min in the flow of 1.05% H_2/He mixture.

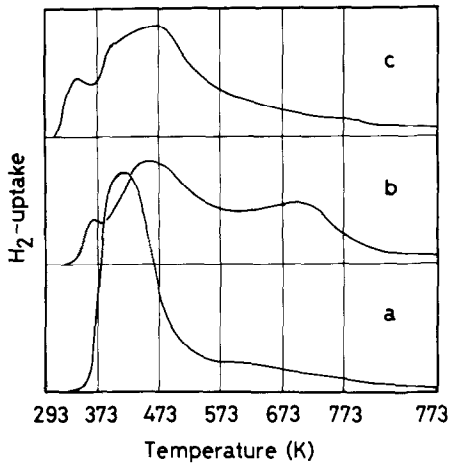

FIG. 10. Effect of calcination temperature on the TPR spectra of catalyst C. (a) Calcined in O_2 at 673 K; (b) calcined in air at 973 K; (c) after (2), the catalyst was calcined in O_2 at 673 K. Catalyst temperature was ramped at 5 K/min.

phase between Rh and Nb_2O_5 was produced by the calcination of catalyst C in air at 973 K.

X-Ray Diffraction

The X-ray diffraction patterns of the unpromoted and the Nb_2O_5-promoted 5.0 wt% Rh/SiO_2 (catalyst B) are given in Fig. 11. The XRD pattern of the 5.0 wt% Rh/SiO_2 catalyst calcined at 973 K (No. 5) contains only the diffraction peaks of Rh_2O_3, and the peaks of Rh metal appeared after the catalyst was reduced in H_2 at 373 K (No. 6). However, the diffraction patterns of catalyst B calcined at 973 K are more complex. In addition to those peaks corresponding to the Nb_2O_5 phase, new diffraction peaks (2θ = 26.8, 35.3, 53.1) are observed (No. 1 in Fig. 11). As will be discussed later, these new peaks may be attributed to the diffraction of the complex oxide of $RhNbO_4$. It should be noted that only a small diffraction peak of the Rh_2O_3 phase was observed after the calcination at 973 K (No. 1). This may be interpreted as a consequence of the reaction between Rh_2O_3 and Nb_2O_5 to form the new phase ($RhNbO_4$). After the catalyst was reduced at 373 K, the new peaks did not exhibit any reduction (No. 2), but these peaks disappeared after HTR at 773 K with the appearance of Rh metal (No. 3). For the catalyst calcined at 673 K after the new phase had been once reduced to Rh, no significant peaks corresponding to $RhNbO_4$ were observed (No. 4). A higher calcination temperature is needed for the formation of the new phase which can be detected by the X-ray diffraction. Moreover, it may be noted that the calcination at 673 K was insufficient to produce the Rh_2O_3 crystal which is detectable by the XRD technique.

The XRD analyses were also performed for the 5.0 wt% Rh/SiO_2 and catalyst B calcined at 773 K. For both catalysts, only the Rh_2O_3 phase was observed. No peaks due to the Nb_2O_5 phase were observed for catalyst B calcined at 773 K. This means that the Nb_2O_5 promoter is well dispersed or it is amorphous.

DISCUSSION

Catalyst A (Nb/Rh = 9.3) contains 5.7 wt% Nb_2O_5 as a promoter. Since no diffraction peaks corresponding to the Nb_2O_5

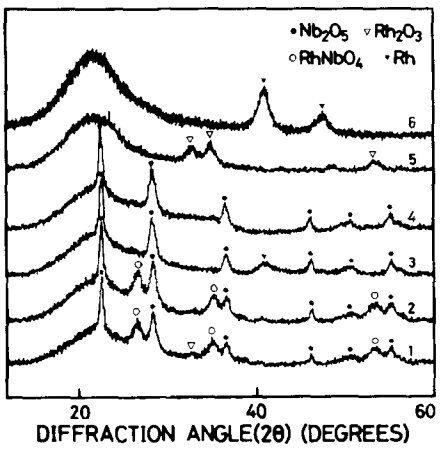

FIG. 11. X-ray diffraction patterns of the unpromoted and Nb_2O_5-promoted Rh/SiO_2 (catalyst B) catalysts. (1) Catalyst B calcined in air at 973 K; (2) after (1), the catalyst was treated in H_2 at 373 K; (3) after (1), the catalyst was reduced in H_2 at 773 K; (4) after (3), the catalyst was treated in O_2 at 673 K; (5) the 5.0% Rh/SiO_2 catalyst calcined in air at 973 K; (6) after (5), the 5.0% Rh/SiO_2 catalyst was reduced in H_2 at 373 K.

phase were observed, the Nb_2O_5 promoter may be either well dispersed over the SiO_2 surface or amorphous. According to the assumption that the Nb_2O_5 promoter is dispersed monolayerly and that each $NbO_{2.5}$ unit mesh in the niobia layer occupies a surface area of 16 $Å^2$ (*17*), about 22% of the SiO_2 surface would be covered by the monolayer niobia in catalyst A (Nb/Rh = 9.3). On the basis of the same assumption, the monolayer niobia coverage of the SiO_2 surface would be 2 and 70% for the catalyst A with an Nb/Rh value of 0.9 and catalyst B, respectively. The results of H_2 chemisorption and Rh dispersion in Table 1 suggest that a part of the deposited Nb_2O_5 may be present on the Rh surface. The Nb_2O_5 promoter on the Rh surface may play an important role in severe suppression of both the H_2 chemisorption capacity and the ethane hydrogenolysis activity after HTR. However, it should also be noted that a large part of the deposited Nb_2O_5 should be on the SiO_2 support, since the Nb/Rh ratio was much greater than 1 for the Nb_2O_5-promoted Rh catalysts which exhibited the SMSI behavior.

The observed SMSI behavior in the Nb_2O_5-promoted Rh/SiO_2 catalysts is very similar to that in the Rh/Nb_2O_5 catalysts (*21*). The activity change of the ethane hydrogenolysis reaction with reduction temperature is very similar between both the Rh/Nb_2O_5 and the Nb_2O_5-promoted Rh/SiO_2 systems, and the activation energy appeared to be almost constant among the data at different catalyst reduction temperatures. Similar results have also been reported on the Rh/TiO_2 catalysts (*27*). Because of the parallel behavior between the present system and the Rh/Nb_2O_5 (*21*) system, the severe suppression in the H_2 chemisorption capacity and the catalytic activity of the Nb_2O_5-promoted Rh/SiO_2 catalysts after HTR may also be caused by the blockage of the surface Rh atoms with NbO_x species formed from the Nb_2O_5 promoter during the high-temperature reduction (decoration model) (*3–9*).

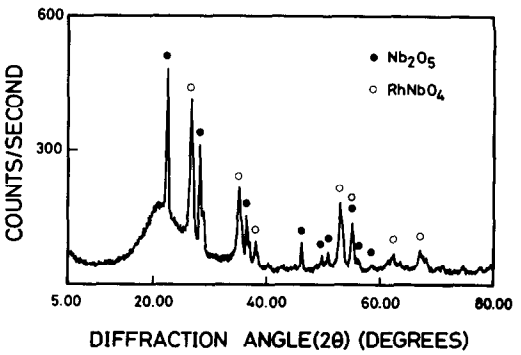

FIG. 12. X-ray diffraction pattern of the Nb_2O_5-promoted 5.0 wt% Rh/SiO_2 catalyst after being calcined in air at 1173 K.

Effect of Calcination at High Temperatures

The new diffraction peaks (*d* values: 3.32, 2.53, 1.72) appeared in the XRD pattern when the Nb_2O_5-promoted Rh/SiO_2 catalyst was calcined in air at 973 K. In order to make an analysis of this new phase, the catalyst was further calcined in air at 1173 K. As shown in Fig. 12, the other peaks in addition to the three main peaks became clear. A best fit was obtained if we calculated the *d* spacing values by assuming the tetragonal $FeNbO_4$ structure (see Table 2). Therefore, it may be considered that the new diffraction peaks correspond to the formation of $RhNbO_4$ compounds.

There is a positive correlation between the calcination treatment and the extent of

TABLE 2

Observed and Calculated *d* Spacing Values (Å) for the New Phase in Fig. 12

Observed *d* values	3.321	2.534	2.355	1.725	1.662	1.485	1.392
I/I_1	100	50	22	47	35	15	18
h k l	110	101	200	211	220	310	301
Calculated *d* values[a]	3.321	2.534	2.349	1.723	1.661	1.485	1.389

[a] The *d* spacing values were calculated by assuming that the new phase takes the tetragonal structure of $FeNbO_4$ (from the standard ASTM XRD values). The *a* and *c* values were calculated to be 4.697 and 3.010 Å, respectively.

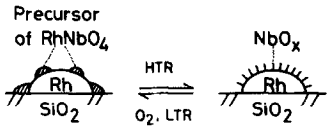

FIG. 13. A model for the SMSI behavior in the Nb_2O_5-promoted Rh/SiO_2 catalysts.

the Rh–Nb_2O_5 interaction; i.e., the calcination of the Nb_2O_5-promoted Rh catalysts in air at 973 K resulted in more severe suppression in the H_2 chemisorption capacity and the ethane hydrogenolysis activity by HTR at 773 K. This result may suggest that the $RhNbO_4$ compound detected by XRD (or its precursor) plays an important role in the decoration of the Rh surface; the formation of $RhNbO_4$ during the calcination treatment may provide a driving force for a more intimate contact between Rh and Nb_2O_5. During the calcination process, those niobia in the vicinity of the Rh particles and/or on the SiO_2 surface may migrate toward the Rh particles at the calcination temperature. The amount of the movable niobia may depend on parameters such as calcination temperature, strength of Nb_2O_5–SiO_2 interaction, and the total amount of the Nb_2O_5 promoter.

The TPR results in Figs. 9 and 10 showed that the calcination treatment at the higher temperature leads to the increase in the contribution of the reduction peaks at the higher temperatures (i.e., more strongly interacting phase between Rh and Nb_2O_5). This phase may correspond to the $RhNbO_4$ compound (or the precursor of $RhNbO_4$). The TPR results are also consistent with the XRD observation (in Fig. 11) that the $RhNbO_4$ compound (formed by the calcination at 973 K) was not reduced by LTR at 373 K, but reduced to the Rh metal by HTR at 773 K. It may be noted that a small contribution from the Rh_2O_3 phase was observed in the XRD pattern in Fig. 11 (No. 1) after the calcination of catalyst B at 973 K. As shown in Fig. 9b, the TPR peak at ca. 430 K may correspond to the reduction of the Rh_2O_3 phase. However, the calcination treatment at 1173 K resulted in the formation of a well-defined phase of $RhNbO_4$, and almost no peaks of the Rh_2O_3 phase were observed in the XRD pattern in Fig. 12.

A Model of Rh–Nb_2O_5 Interaction

In the Nb_2O_5-promoted Rh/SiO_2 catalysts used in this study, it was suggested that the Rh surface was partially covered with the Nb_2O_5 promoter even after the O_2 treatment at 673 K followed by LTR at 373 K. Moreover, the degree of the Rh–Nb_2O_5 interaction increased as the contribution of the reduction peak at the higher-temperature side increased in the TPR spectra (see Figs. 7, 9, and 10). The TPR peak at the higher-temperature side was related to the reduction of the $RhNbO_4$ compound (or its precursor). The O_2 treatment at 673 K may be insufficient to produce the $RhNbO_4$ phase, since no diffraction peaks of $RhNbO_4$ were found after this treatment of the catalyst B (Fig. 11). However, it would not exclude the possible formation of the $RhNbO_4$ precursor (which is undetectable by the XRD technique). From these results, we propose a probable model for the SMSI behavior, as shown in Fig. 13. A precursor of $RhNbO_4$ (or the surface $RhNbO_4$ compound) may be produced by the O_2 treatment at 673 K. After LTR, Rh oxide is reduced to the Rh metal, but the surface $RhNbO_4$ compound remains unreduced. As presented in Fig. 13, an island-like decoration may be considered, based on the assumption that part of the Rh surface is exposed after LTR, since the catalyst after LTR has a hydrogen chemisorption capacity and a high activity of the ethane hydrogenolysis reaction. The surface $RhNbO_4$ compound is reduced by HTR at 773 K, and the Rh surface may be covered uniformly with Nb oxide species (NbO_x), which results in the state of the severely suppressed H_2 chemisorption capacity and catalytic activity (a geometric effect) (*3, 4, 20, 21*).

The observed results may be explained qualitatively by this model. However, it

should be pointed out that the detailed mechanism in this catalyst system is not yet clear at the present stage. One interesting point is that no exact parallel correlation between the behaviors of the H_2 chemisorption and the ethane hydrogenolysis activity was observed with changing the reduction temperature (see Figs. 1–3, 5, and 6). In most of the Nb_2O_5-promoted Rh catalysts, the H/Rh value decreased severely even after the H_2 reduction at 573 K, but the ethane hydrogenolysis activity was not decreased significantly by the H_2 reduction at this intermediate temperature. It may be concluded that the ethane hydrogenolysis activity is severely suppressed when the H/Rh value decreased to almost zero after HTR at 673–773 K. More complicated structural changes and/or electronic interaction might be considered in order to elucidate the detailed mechanism for the above results. Ko *et al.* have developed a hierarchy consisting of five steps to rank the extent of interaction in Ni/Nb_2O_5 catalysts for the interpretation of their results by the chemical probes such as CO hydrogenation, ethane hydrogenolysis, and H_2 chemisorption (*17, 28*). However, the detailed interpretation in the present catalyst system will be the subject of further investigation.

ACKNOWLEDGMENTS

One of the authors (Z. Hu) thanks Tianjin University, China. This work was supported in part by a Grant-in-Aid for Scientific Research from the Ministry of Education, Science and Culture, Japan.

REFERENCES

1. Tauster, S. J., Fung, S. C., and Garten, R. L., *J. Amer. Chem. Soc.* **100,** 170 (1978).
2. Tauster, S. J., Fung, S. C., Baker, R. T. K., and Hourseley, J. A., *Science* **211,** 1121 (1981).
3. Resasco, D. E., and Haller, G. L., *J. Catal.* **82,** 279 (1983).
4. Haller, G. L., Henrich, V. E., McMillan, M., Resasco, D. E., Sadeghi, H. R., and Sakellson, S., "Proceedings, 8th International Congress on Catalysis, Berlin, 1984," Vol. V, p. 135. Dechema, Frankfurt-am-Main, 1984.
5. Sadeghi, H. R., and Henrich, V. E., *J. Catal.* **87,** 279 (1984).
6. Takatani, S., and Chung, Y. W., *J. Catal.* **90,** 75 (1984).
7. Ko, C. S., and Gorte, R. J., *J. Catal.* **90,** 59 (1984).
8. Belton, D. N., Sun, Y.-M., and White, J. M., *J. Phys. Chem.* **88,** 5172 (1984).
9. Raupp, G. P., and Dumesic, J. A., *J. Catal.* **95,** 587 (1985).
10. Ichikawa, M., Fukushima, T., and Shikakura, K., "Proceedings, 8th International Congress on Catalysis, Berlin, 1984," Vol. 2, p. 69. Dechema, Frankfurt-am-Main, 1984.
11. Bhasin, M. M., Bartley, W. J., Ellgen, P. C., and Wilson, T. C., *J. Catal.* **54,** 120 (1978).
12. Ichikawa, M., and Fukushima, T., *J. Phys. Chem.* **89,** 1564 (1985).
13. Pande, N. K., and Bell, A. T., *J. Catal.* **97,** 137 (1986).
14. Rieck, J. S., and Bell, A. T., *J. Catal.* **99,** 262 (1986).
15. Rieck, J. S., and Bell, A. T., *J. Catal.* **99,** 278 (1986).
16. Singh, A. K., Pande, N. K., and Bell, A. T., *J. Catal.* **94,** 422 (1985).
17. Ko, E. I., Bafrali, R., Nuhfer, N. T., and Wanger, N. J., *J. Catal.* **95,** 260 (1985).
18. McViker, G. B., and Ziemiak, J. J., *J. Catal.* **95,** 473 (1985).
19. Lin, Y.-J., Resasco, D. E., and Haller, G. L., *J. Chem. Soc. Faraday Trans. 1* **83,** 2091 (1987).
20. Kunimori, K., Doi, Y., Ito, K., and Uchijima, T., *J. Chem. Soc. Chem. Commun.*, 966 (1986).
21. Kunimori, K., Ito, K., Iwai, K., and Uchijima, T., *Chem. Lett.*, 573 (1986).
22. Kunimori, K., Hu, Z., Ito, K., Maeda, A., Nakamura, H., and Uchijima, T., *Shokubai (Catalyst)* **29,** 106 (1987); "59th CATSJ Meeting Abstracts," No. A16. 1987.
23. Murakami, Y., *in* "Preparation of Catalysts III" (G. Poncelet, P. Grange, and P. A. Jacobs, Eds.), p. 775. Elsevier, Amsterdam, 1983; *Shokubai (Catalyst)* **26,** 280 (1984).
24. Kunimori, K., Ikeda, Y., Soma, M., and Uchijima, T., *J. Catal.* **79,** 185 (1983).
25. Haller, G. L., Resasco, D. E., and Rouco, A. J., *Faraday Discuss. Chem. Soc.* **72,** 109 (1981).
26. Kunimori, K., Hashimoto, T., Ito, S., and Uchijima, T., *Denki Kagaku* **54,** 868 (1986).
27. Resasco, D. E., and Haller, G. L., *in* "Studies in Surface and Catalysis" (B. Imelik, *et al.*, Eds.), Vol. 11, p. 105. Elsevier, Amsterdam, 1982.
28. Ko, E. I., Hupp, J. M., and Wanger, N. J., *J. Catal.* **86,** 315 (1984).